Applied Surface Science 518 (2020) 146269

Contents lists available at ScienceDirect

Applied Surface Science

journal homepage: www.elsevier.com/locate/apsusc

Full Length Article

Surface density dependent orientation and immunological recognition of antibody on silicon: TOF-SIMS and surface analysis of two covalent immobilization methods

Katarzyna Gajos[a,*], Klaudia Szafraniec[a], Panagiota Petrou[b], Andrzej Budkowski[a,*]

[a] M. Smoluchowski Institute of Physics, Jagiellonian University, Łojasiewicza 11, 30-348 Kraków, Poland
[b] Institute of Nuclear & Radiological Sciences & Technology, Energy & Safety, NCSR Demokritos, P. Grigoriou & Neapoleos St, Aghia Paraskevi 15341, Athens, Greece

ARTICLE INFO

Keywords:
TOF-SIMS
AFM
Antibody orientation
Antibody immobilization
Antigen binding efficiency
Random sequential adsorption

ABSTRACT

Antibodies are commonly used as detection elements in biosensors. Antibody orientation on transducer surface determines immunological recognition and biosensor performance. Although a relation between antibody orientation and adsorbed amount Γ was predicted, assuming close packing of proteins, and even applied to infer the preferred orientation from indirect surface analysis, the issue has not been so far examined experimentally with the surface techniques probing *directly* antibody orientation for a wide Γ range covering all possible antibody orientations. In this work, time-of-flight secondary ion mass spectrometry combined with Principal Component Analysis probes the orientation of immunoglobulin G (aIgG) immobilized on silane-modified silicon surface with surface density $0 \leq \Gamma \leq 3$ mg/m^2, determined with ellipsometry. Two covalent immobilization methods: with NHS-silane and with amino-silane followed by glutaraldehyde (GA) activation, are compared. Atomic Force Microscopy reveals surface density dependent nanostructure of aIgG layers. AFM and PCA of TOF-SIMS clearly distinguish between the Γ ranges of flat-on, side-on and vertical aIgG orientation, that accord with random molecular packing. For vertical aIgG arrangement, a dominant head-on orientation and a mixed tail-on/head-on orientation is concluded from PCA for GA- and NHS-surface modification, respectively. In addition, molar binding ratio of antigen to antibody accords with the determined surface density dependent aIgG orientation.

1. Introduction

Immunosensors employing antibodies as capture molecules are one of the most powerful biosensors type applicable in areas ranging from biomedical diagnostic to food safety and drug screening [1,2]. Regardless of the type of the detection system, including electrochemical, optical, piezoelectric and magnetic detection, immunosensor development requires the immunoreagents immobilization on transducers surface paying attention to dependence of sensors analytical performance on the orientation and amount of surface-immobilized molecules [2,3]. In the case of immunoglobulins G (IgG), described by characteristic three lobe (Y)-shaped domains with one Fc domain and two Fab domains (where antigen binding sites are located), four different antibody orientations on the surface can be distinguished, i.e. flat-on (all three lobes attached to surface), side-on (Fc and one Fab at substrate), head-on (Fc-up and both Fabs attached to surface) and tail-on (Fc at surfaces and both Fabs-up), resulting in different access to binding sites and antigen binding efficiency [3]. To control orientation of antibodies on the surface different non-covalent, covalent and affinity immobilization approaches were developed [3,4]. When antibody undergoes physisorption, even prior to other different surface conjugation events [3], its orientation can be controlled by a molecular-scale physical interactions, involving electrostatic and hydrophobic forces [5–8]. Additionally, the surface density Γ of antibodies determines possible orientations since decreasing surface area accessible to each molecule forces its more vertical orientation [8,9]. A simple relation between Γ and orientation, assuming highly ordered close packing of proteins, was predicted by Norde [8].

Determination of antibodies orientation on surface is of fundamental interest. Recently, surface-immobilized antibodies orientation is most commonly inferred from the antibodies surface density Γ [3,8] or amount of bound antigen [4], determined with different surface analysis techniques such as spectroscopic methods [5,10,11] or quartz crystal microbalance [9,12]. However, it is an *indirect* approach prone

* Corresponding authors.
E-mail addresses: katarzyna.gajos@uj.edu.pl (K. Gajos), andrzej.budkowski@uj.edu.pl (A. Budkowski).

https://doi.org/10.1016/j.apsusc.2020.146269
Received 19 January 2020; Received in revised form 20 March 2020; Accepted 30 March 2020
Available online 30 March 2020

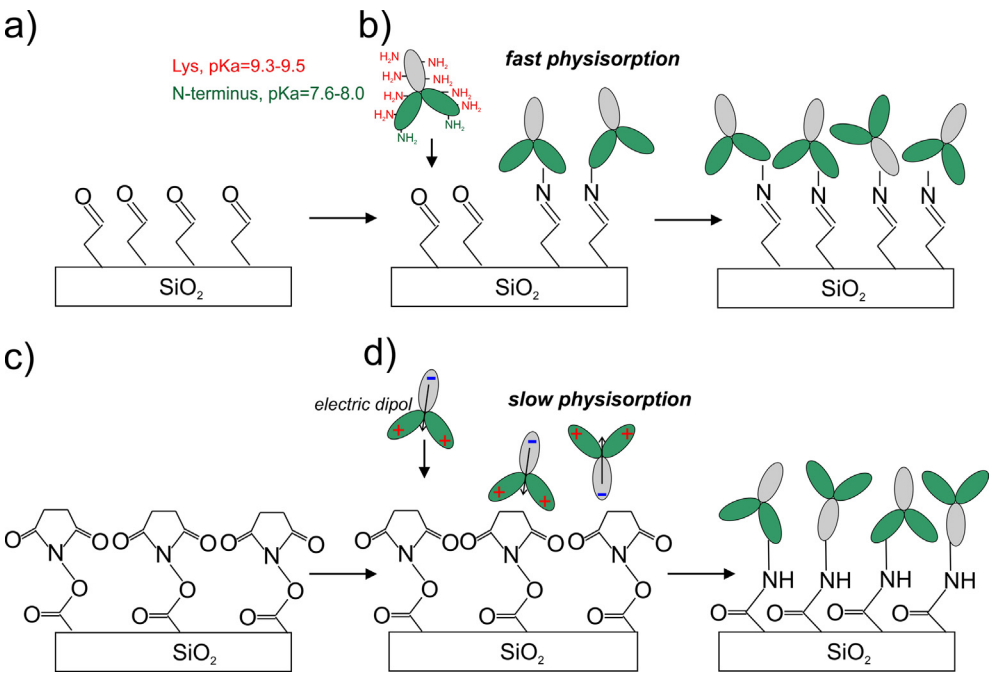

Scheme 1. Schematic of SiO_2 surface modified with APTES and glutaraldehyde (a) or with NHS-silane (c). Diagrams showing the mechanism of covalent attachment of aIgG to those surfaces and aIgG orientation onto APTES/glutaraldehyde (b) and NHS-silane (d) modified surfaces in case of high protein surface density corresponding to vertical molecules' orientation.

to high uncertainty related to ambiguities of orientations for same Γ ranges or protein packing on surface. In turn, Atomic Force Microscopy has been applied to deduce orientation of antibodies based on the determination of the dimensions of single molecules [13,14] or thickness of the antibodies layer [5,15]. Apart from the mentioned approaches, Time-of-Flight Secondary Ion Mass Spectrometry (TOF-SIMS) enables a *direct orientation analysis* of surface-immobilized antibodies [6,16–21], based on the differences in amino acid composition between antibodies domains and a limited emission (attenuation) depth λ of about 1 nm, corresponding to outermost region of molecules adsorbed on surface. Due to a great complexity of TOF-SIMS data a multivariate statistical analysis with Principal Component Analysis [6,17–19,22] or artificial neural network [18] is normally applied to enhance capturing subtle differences in data set.

For silicon-based immunosensors, suitable for development of point-of-need platforms due to well-established and cost-efficient fabrication processes [23,24], the transducer surface should be appropriately functionalized prior to the immobilization of immunoreagents. Surface modification with silanes forming self-assembled monolayers and enabling a protein covalent binding or enhancing its physical adsorption is here a simple and effective approach. However, the performed so far analysis of antibodies orientation on SAM layers was limited to thiol-modified gold substrates [5,6,17] and moreover did not take into account the surface density of immobilized antibodies.

In this work, TOF-SIMS spectrometry with Principal Component Analysis is employed to *determine directly the orientation* of surface-immobilized goat anti-rabbit IgG (aIgG) *as a function of antibodies surface density*, which was not reported earlier. Additionally, AFM analysis reveals surface density dependent nanostructure of aIgG layers. The proposed approach enables an estimation of the ranges of the mass loading corresponding to flat-on, side-on and vertical (head-on vs. tail-on) aIgG orientation, that accord with packing efficiency characteristic for random sequential adsorption. Also, the antigen binding efficiency reflecting different antibodies orientation is examined for the whole range of aIgG mass loading to provide optimal conditions of aIgG immobilization for immunodetection. Surface density dependent aIgG orientation is analyzed and compared on silicon surfaces modified following two popular methods enabling covalent antibodies binding: functionalization with NHS-ester groups (by silanization with NHS-silane) and aldehyde groups (by silanization with amino-silane and activation with glutaraldehyde). Different antibody orientation mechanisms, related with physisorption and chemisorption, are relevant for both immobilization methods.

2. Experimental

2.1. Silicon surface modification with silanes

Silicon substrates with a native SiO_2 layer (Si-Mat, GmbH, Germany) were cleaned by sonication in toluene (POCh, Gliwice, Poland) and ethanol (POCh, Gliwice, Poland), sequentially, for 10 min. Then substrates were cleaned and hydrophilized by treatment in oxygen plasma for 30 s. The surface functionalization with NHS-ester was performed through immersion of cleaned silicon substrate in a 1 mg/mL 5-(chlorodimethylsilanyl)-pentanoic acid 2,5-dioxo-pyrrolidin-1-yl ester (NHS-silane) (ProChimia, Gdańsk, Poland) solution in toluene for 1 h, followed by washing in sequence with toluene and ethanol in ultrasonic bath and drying under a stream of nitrogen. The effective surface modification was confirmed by the increase of water contact angle up to 60° and measurements of the silane layer thickness with spectroscopic ellipsometry (0.4(± 0.1) nm). In turn, for surface functionalization with aldehyde groups substrates were silanized through immersion in a 1% (v/v) 3-aminopropyltriethoxysilane (APTES) (Sigma-Aldrich, Darmstadt, Germany) solution in toluene for 10 min, followed by washing with toluene and ethanol in ultrasonic bath, drying under a stream of nitrogen and backing for 20 min at 120 °C. After that, the APTES modified substrates were immersed in a 2.5% (v/v) aqueous glutaraldehyde solution for 20 min, followed by washing with distilled water and drying under nitrogen stream. The determined with spectroscopic ellipsometry thickness of APTES layer activated with glutaraldehyde was 1.2(± 0.1) nm and water contact angle was about 55°.

2.2. Immunoglobulin G immobilization and immunoassay

The polyclonal goat anti-rabbit antibody (aIgG) (Thermo Fisher Scientific, Rockland, USA) was immobilized by covalent binding on silicon surface functionalized with NHS-silane Scheme 1c and APTES activated with glutaraldehyde Scheme 1a. To obtain various aIgG surface densities, functionalized silicon substrates were incubated with

solutions of aIgG in 0.15 M phosphate buffer saline (Sigma-Aldrich, Darmstadt, Germany), pH 7.4, with concentrations ranging from 5 μg/mL to 1 mg/mL for 30 min, followed by washing with phosphate buffer saline. Additionally, for the reference surfaces, $F(ab)_2$ and Fc fragments of aIgG were immobilized on functionalized silicon substrates from a solution with concentration 500 μg/mL. Prior to characterization with surface science techniques all samples were washed with distilled water and dried under nitrogen stream. Protein surface density was determined with spectroscopic ellipsometry on each individual sample.

To determine the antigen binding efficiency of surface-immobilized aIgG a reaction with polyclonal rabbit IgG (rIgG) (Sigma-Aldrich, Darmstadt, Germany) was performed for surfaces with various antibody surface density. For this purpose, immediately after aIgG immobilization, the substrates were blocked with bovine serum albumin (BSA) (ACROS Organics, Geel, Belgium) through incubation with a 2 mg/mL BSA solution in 0.15 M phosphate buffer saline for 30 min. After gently washing with phosphate buffer, the samples were incubated with a 10 μg/mL rIgG solution in phosphate buffer saline for 30 min, followed by washing with buffer, distilled water and drying under nitrogen stream. To determine the molar binding ratio of rIgG to aIgG, the protein surface density was determined with spectroscopic ellipsometry on silanized silicon surfaces after aIgG immobilization, blocking with BSA, and reaction with rIgG for each one of the antibody concentration used for coating of the surfaces.

2.3. Surface density determination with spectroscopic ellipsometry

The Sentech SE800 (Sentech Instruments GmBH) Spectroscopic Ellipsometer was employed to perform spectroscopic ellipsometry measurements over a wavelength range of 320–700 nm and at a fixed incidence angle equal to 70°. Results were analyzed with the SpectraRay 3 software. For the estimation of the average thickness of silane and protein layer the Cauchy dispersion model was assumed and the two-layer model consisted of silicon substrate/mixed SiO_2 and silane/protein layer was applied. Fixed refractive index values equal to n = 3.87 for Si, n = 1.46 for SiO_2, NHS-silane, APTES and glutaraldehyde [25], and n = 1.53 [26] for protein were used. A constant thickness of 2.7 nm for the SiO_2 layer, obtained from fitting measurements performed on plasma cleaned silicon surfaces, was taken into account to fit the thickness of silane and protein layers. The thickness of silane layers determined for bare silane-modified silicon substrates equals to 0.4(± 0.1) nm for NHS-silane and to 1.2(± 0.1) nm for APTES activated with glutaraldehyde. These values were taken as constants to fit the thickness d of protein layer. The protein surface density Γ was estimated following the Cuypers one-component approach: $\Gamma = d*\rho = d*(M/A)*(n_p^2-1)/(n_p^2+2)^2$ [27]. A value of refractive index, $n_p = 1.53$ [26], and a ratio of molecular weight to molar refractivity, M/A = 4.14 g/mL [27] are assumed for all the proteins [26,27].

2.4. AFM characterization

Topography AFM images of protein layers on silicon surfaces modified with silanes were recorded with an Agilent 5500 microscope working in non-contact mode. AFM probes with spring constant about 2 N/m, tip radius about 7 nm and resonant frequencies about 70 kHz were used. For each sample, several AFM micrographs were taken at different areas. The WSxM software provided by Nanotec Electronica S.L. [28] (downloadable at http://www.nanotec.es) was applied for the analysis of AFM images and determination of nanostructure parameters.

2.5. TOF-SIMS characterization

TOF-SIMS analysis was conducted using the TOF.SIMS 5 (ION-TOF GmbH) instrument equipped with Bi_3^+ ion clusters (30 keV liquid metal ion gun). Ion dose density about 10^{12} ion/cm^2, corresponding to static mode, and current about 0.5 pA were applied to all measurements. A low energy electron flood gun was used for charge compensation. Positive ion high mass resolution TOF-SIMS spectra were acquired from ten non-overlapping 100 μm × 100 μm (applied resolution was 128 × 128 points) areas of each sample. Mass calibration was performed with H^+, H_2^+, CH^+, $C_2H_2^+$ and $C_4H_5^+$ peaks. A minimal mass resolution (m/Δm) > 8000 at $C_4H_5^+$ was obtained.

2.6. Multivariate TOF-SIMS analysis with PCA

Principal Component Analysis was performed for the positive TOF-SIMS spectra using the PLS Toolbox (Eigenvector Research, Manson, WA) for MATLAB (MathWorks, Inc., Natick, MA). The intensities of selected peaks from each spectrum were normalized to the sum of selected peaks and mean-centred before running PCA.

3. Results and discussion

3.1. aIgG immobilization on silane layers

To obtain samples with different surface density of immobilized antibody various concentrations (ranging from 5 to 1000 μg/mL) of aIgG solution were applied onto the SiO_2 surfaces modified with two different silanes, amino-silane (APTES) and NHS-silane, the former after activation with glutaraldehyde. The aIgG immobilization resulted in antibody surface density Γ in the range 0.7–3.0 mg/m^2 [and corresponding areal number density N/S = (2.8–12) × 10^3 μm^{-2})] for APTES/glutaraldehyde (GA) modified surfaces and 0.2–2.8 mg/m^2 [N/S = (0.8–11.2) × 10^3 μm^{-2}] for NHS-silane modified surfaces, as determined with Spectroscopic Ellipsometry. Adsorption isotherms for both surface functionalization approaches are presented in Fig. 1. Data points were described using two adsorption models, namely (extended) Langmuir model [29] and Random Sequential Adsorption (RSA) model [30,31] (for the details see Section S1 in Supplementary Material), providing adsorption parameters such as binding capacity (BC) and affinity constant (AF). Both models calculate higher binding capacity values for APTES/glutaraldehyde rather than NHS-silane modified surfaces (~3.3 mg/m^2 vs. ~2.7 mg/m^2 from Langmuir model, and BC ~3.8 mg/m^2 vs. ~3.2 mg/m^2 from RSA model). These results are in accordance with previously reported results for streptavidin, showing

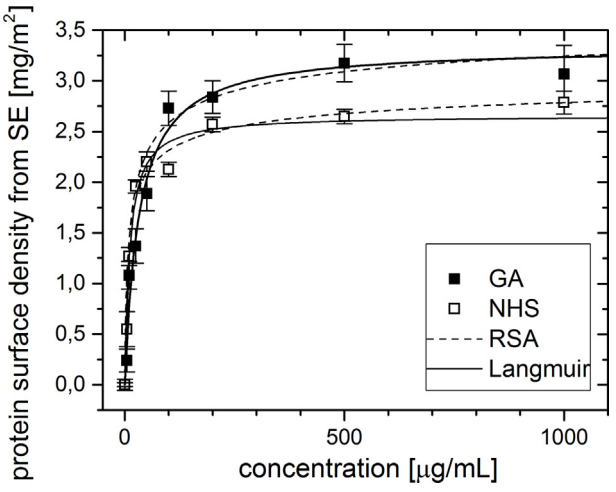

Fig. 1. Adsorption isotherms of goat anti-rabbit IgG antibody (aIgG) on silicon surfaces functionalized with APTES and activated by glutaraldehyde (GA, black squares) or NHS-silane (open squares), respectively. The protein surface density was determined with spectroscopic ellipsometry. Lines describe experimental data on basis of Langmuir model (solid line) and RSA model (dashed line), respectively.

higher binding capacity to aldehyde than NHS-ester modified glass surfaces [32]. In turn, the affinity constant is higher for NHS-silane than APTES/glutaraldehyde modification (~1.4 * 10^7 1/M vs. ~0.5 * 10^7 1/M from Langmuir model, and BC ~2.8 * 10^7 1/M vs. ~1.6 * 10^7 1/M from RSA). The values of aIgG surface density determined for both modification approaches for a solution with concentration equal to 100 μg/mL are higher than the values determined previously on silicon surfaces for physical adsorption of IgG on amino-silane ~1.4–1.6 mg/m^2 [33,34] or covalent binding to epoxy-silane modified surfaces ~0.3 mg/m^2 [34].

The determined surface amounts Γ of immobilized aIgG should cover characteristic surface mass densities corresponding to a monolayer of aIgG where the molecules adapt all possible orientations. *Characteristic* mass loadings, related to individual biomolecule Γ_{ind} with different molecular orientations were predicted for highly ordered close packing of proteins, and are 2 mg/m^2 for flat-on orientation, 2.6–5.5 mg/m^2 for tail-on/head-on with spaced (2.6 mg/m^2), intermediate (3.7 mg/m^2), or contracted (5.5 mg/m^2) Fab fragments [8]. However, the packing efficiency of adsorbed proteins (jamming limit, Θ_∞ ~0.55 [31]) is smaller than that of close packed molecules, since due to random sequential adsorption the distance between neighboring proteins is not zero but ranges from zero to molecule diameter [31,35]. Therefore, lower values of characteristic mass loadings, corresponding to ($\Gamma_{ind}\Theta_\infty$), are expected [20,31]: Using the Γ_{ind} data provided for all antibody orientations by molecular dynamics simulations [14], representative amounts of 1.4 mg/m^2 for flat-on (compared with ~ 1.1 mg/m^2 from [8]), 1.9 mg/m^2 for side-on, and 2.2–2.4 mg/m^2 for tail-on/head-on molecular arrangement are calculated. The latter extends to a range 1.4–3.0 mg/m^2 for vertical orientation of antibody molecules depending on the angle between Fab fragments [8].

In addition, to examine a surface sensitivity of TOF-SIMS technique [36,37] the protein surface density determined with ellipsometry was compared with protein surface composition provided by the PCA analysis of TOF-SIMS data (see Section S2 in Supplementary Material). The results obtained reveal the ability of TOF-SIMS to probe the complete protein monolayer ('escape' depth [37] ~3.0 nm corresponds to uniform protein layer with surface density ~3.8 mg/m^2) while demonstrating the higher sensitivity for the outermost region of the protein layer (described by the attenuation depth λ = 0.63 (± 0.10) nm). A detailed discussion is provided in Section S2 in Supplementary Material.

3.2. Characterization of IgG layers with AFM

To provide an insight into nanostructure of aIgG layers prepared on APTES/glutaraldehyde and NHS-silane functionalized SiO_2 substrates, AFM microscopy was employed. Layers of aIgG molecules with various protein surface density as well as reference surfaces covered with $F(ab)_2$ and Fc fragments of aIgG were analyzed. In Fig. 2a-b representative topographic images of bare functionalized substrates and substrates with aIgG layers corresponding to various surface density values, for which different antibody molecules orientations are expected, are presented. In addition, parameters describing vertical and lateral nanostructure of molecular layers were determined as a function of protein surface amount. Vertical nanostructure is specified by the average height, determined as the mean of the height distribution in the respective AFM image (Fig. S2 in Supplementary Material). In turn, lateral nanostructure is characterized by the mean size of surface features 2whm, provided by the doubled width-at-half-maximum of a radial averaged autocorrelation function computed for each AFM image (Fig. 2c).

An analysis of AFM data indicates uniformity of molecules distribution for all surfaces. SiO_2 substrates functionalized with APTES/glutaraldehyde or NHS-silane are characterized by an average height of about 0.8–0.9 nm and surface roughness of about 0.3 nm, that accords with values determined previously for SiO_2 and Si_3N_4 substrates functionalized with silane monolayers [20,33,34,38]. In turn, the mean size of surface features is about 15 nm and 13 nm for APTES/glutaraldehyde and NHS-silane modified surfaces, respectively (Fig. 2c).

For the surface-immobilized aIgG molecules the layer's average height increases with the protein surface density (Fig. S2), reflecting both orientation changes and an increase in the amount of surface features. In turn, the changes of features size are not monotonic and are following subsequent changes of the molecules orientation (Fig. 2c). To analyze these changes test measurements were performed for a single antibody lobe (Fc) and a pair of lobes ($F(ab)_2$), yielding apparent feature size of ~15 nm and ~20 nm, respectively. For aIgG layers with low mass loading, for which the flat-on orientation is expected (marked as I in Fig. 2c), the determined feature size is of about ~20 nm. This value is higher than that for bare silane-modified surfaces (13–15 nm). Also, it reflects the exposed paired lobes of aIgG molecule (~20 nm) as dominant surface features resolved during AFM examination. An increase of surface density above 1.2 mg/m^2 results in pronounced reduction of the surface features size to 14–17 nm. This is regarded as a token of antibody rearrangement into side-on orientation, expected for higher mass loadings (1.2–2.2 mg/m^2, marked as region II), and characterized by an elevated single lobe accessible to AFM (~15 nm). In turn, for even higher surface density (> 2.2 mg/m^2, marked as III) the feature size returns to values above 18 nm, interpreted as arrangement of the molecules into vertical orientation where the paired lobes (~20 nm) are again dominant in AFM analysis.

A similar observation regarding the reduction of the IgG molecules dimensions determined by AFM when adapting side-on orientation compared to flat-on and head-on/tail-on orientations, which is the most prominent feature of Fig. 2c, was reported by Vilhena et al. for an adsorbed IgG molecule [14]. This study revealed stable molecular configurations, visualized by molecular dynamics simulation [14], with a single lobe significantly elevated above the rest of IgG molecule for side-on orientation as compared for other orientations (including head-on arrangement) for which larger fragments of IgG molecule appear elevated [14]. Our results (Fig. 2c), in particular the reduction of mean surface feature size in the region II, seem to support the finding of Vilhena et al. [14], relating the reduction of the determined dimensions of IgG molecules with their side-on orientation.

The features size determined for the aIgG layers (Fig. 2c) accords with the values reported for corresponding protein surface density of IgG molecules adsorbed on silicon substrates with other SAM layers: 16 nm [33,38] – 18 nm [20] for 1.4 mg/m^2, and 23 nm [20] for 2.0 mg/m^2.

3.3. Analysis of aIgG orientation with TOF-SIMS and PCA analysis

To analyze directly dominant aIgG orientation for different protein surface densities, PCA analysis of TOF-SIMS data was employed. In this analysis, 33 positive ion fragments characteristic for amino acids [39] (and listed in Fig. 5) were examined to detect subtle differences in amino acid composition of the outmost region of immobilized aIgG molecules adopting different orientations. The PCA model was developed including TOF-SIMS data recorded from reference samples of bare modified silicon substrate and substrates with immobilized $F(ab)_2$ and Fc fragments, as well as aIgG overlayers characterized by surface density values corresponding to three different expected molecules orientations: I – flat-on orientation (0.2 ± 0.1 mg/m^2 and 0.6 ± 0.2 mg/m^2 for APTES/glutaraldehyde and NHS-silane modification, respectively), II – side-on orientation (1.4 ± 0.1 mg/m^2 for APTES/glutaraldehyde and 2.0 ± 0.2 mg/m^2 for NHS-silane modification) and III – vertical orientation (3.1 ± 0.1 mg/m^2 and 2.8 ± 0.2 mg/m^2 for APTES/glutaraldehyde and NHS-silane modification, respectively). Since to some TOF-SIMS signals characteristic for protein the contributions from the substrate are expected, the main source of the TOF-SIMS intensities variability in the analyzed dataset, captured by the first principal component (PC1) describing the majority

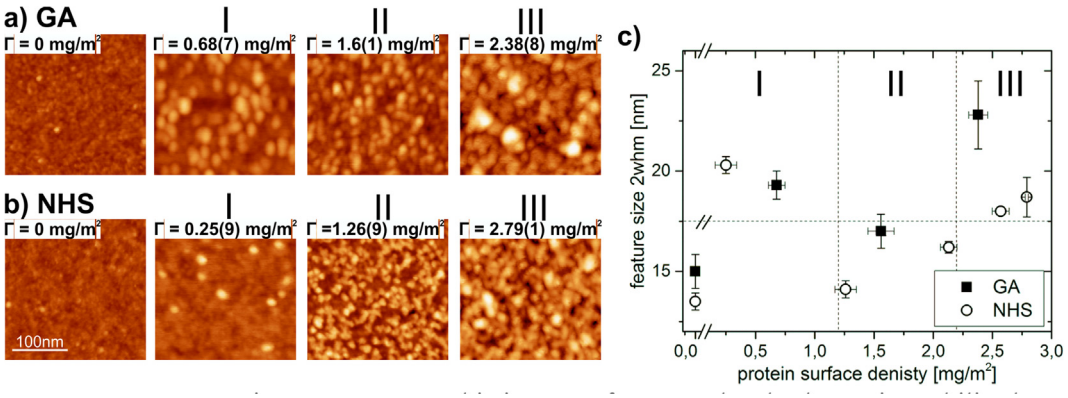

Fig. 2. Representative AFM topographic images of aIgG molecules layers immobilized on SiO_2 substrates functionalized with APTES/glutaraldehyde (GA) (a) or NHS-silane (b) with different surface density corresponding to different aIgG orientation: I – flat-on, II – side-on and III – vertical orientation. (c) The mean size of surface features, 2whm, determined from AFM images reflecting changes in aIgG molecules orientation. An identical height-range of 6 nm is applied for all images. Error bars are standard deviations determined from 4 AFM images of the same sample.

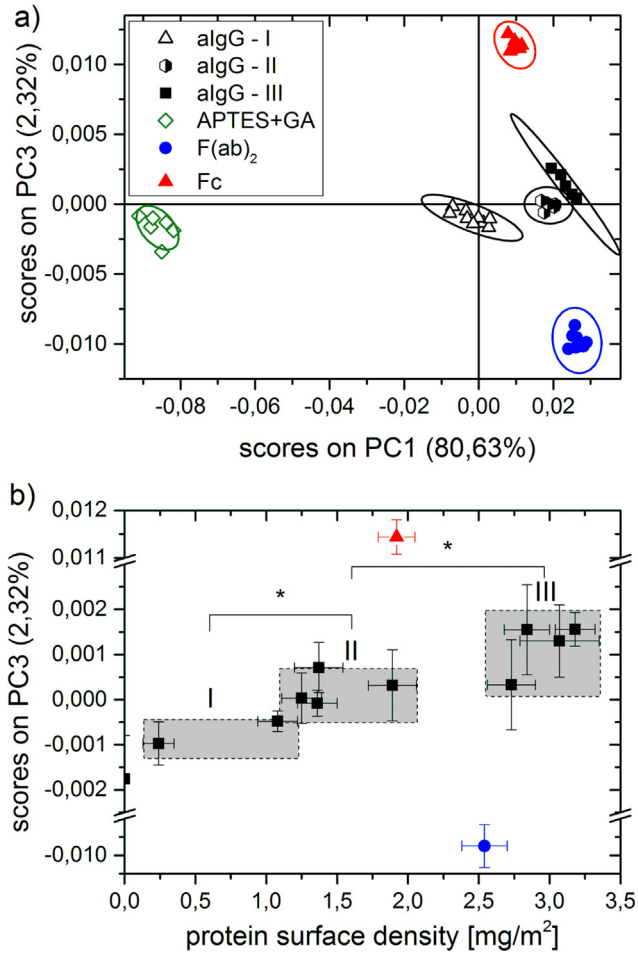

Fig. 3. aIgG molecules orientation analysis with PCA of TOF-SIMS data for surface functionalization with APTES/glutaraldehyde. (a) PC1 vs. PC3 scores plot for the developed PCA model involving bare substrate, representative aIgG layers with surface density corresponding to different aIgG orientations (I – flat-on, II - side-on and III – vertical orientation), as well as surfaces coated with F $(ab)_2$ and Fc antibody fragments as reference layers. The ellipses drawn around each of the grouped data points represent the 95% confidence limit. (b) Mean values of scores on PC3 versus surface density of aIgG molecules. Three data points groups corresponding to different aIgG orientations (in sequence flat-on, side-on and head-on) can be distinguished (* significantly different of each other, $p < 0.05$). Error bars are standard deviations determined from 6 to 10 TOF-SIMS measurements and 5 ellipsometry measurements of the same sample.

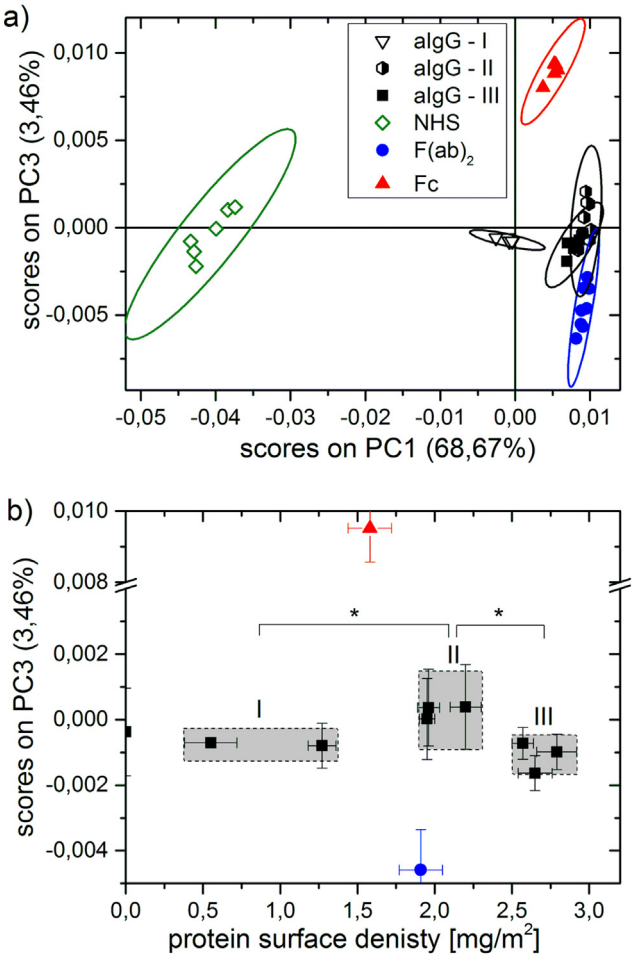

Fig. 4. Orientation analysis of aIgG molecules with PCA of TOF-SIMS data for surface functionalized with NHS silane. (a) PC1 vs. PC3 scores plot for developed PCA model involving bare substrate, representative aIgG layers with surface densities corresponding to different aIgG orientation (I – flat-on, II – side-on and III – vertical orientation), as well as reference surfaces with immobilized F$(ab)_2$ and Fc antibody fragments. The ellipses drawn around each of the grouped data points represent the 95% confidence limit. (b) Mean values of scores on PC3 versus surface density of aIgG molecules. Three data points groups corresponding to different aIgG orientations (in sequence flat-on, side-on and tail-on/head-on) can be distinguished (* significantly different of each other, $p < 0.05$). Error bars are standard deviations determined from 6 to 10 TOF-SIMS measurements and 5 ellipsometry measurements of the same sample.

of the variance, is related to protein surface coverage (Figs. 3a and 4a). Due to the orthogonality of Principal Components, composition changes due to the aIgG orientation, independent from those caused by surface coverage, can be described by one of the further Principal Components uncorrelated to PC1. Then, in order to study the surface density dependent aIgG molecules orientation, the TOF-SIMS data recorded for all surface samples with immobilized aIgG were projected onto the developed PCA model, as it was proposed by Wang et al. [6].

3.3.1. Surface functionalization with APTES and glutaraldehyde modification

The scores plot (PC3 vs. PC1) for the developed PCA model obtained for SiO_2 substrates functionalized with APTES and subsequently activated with glutaraldehyde is shown in Fig. 3a. As discussed above, the PC1, which captures 80.63% of the total variance, separates samples by protein surface coverage. The second principal component capturing 15.63% of variance separates sample with low IgG surface density (0.2 ± 0.1 mg/m^2) from other ones. Since the loadings analysis for this principal component is inconclusive it was no longer considered. In turn, the third principal component, capturing 2.32% of variance uncorrelated to that described by the PC1, differentiates spectra recorded from antibody layers and those from reference samples with immobilized $F(ab)_2$ and Fc fragments. Therefore, the scores values on PC3 can be used as an indicator of aIgG orientation, as the latter specifies exposure of Fc as compared to $F(ab)_2$ antibody domains and defines amino acid composition of the outermost regions of the antibody layer. The PC3 scores values calculated by projection of all TOF-SIMS spectra recorded from surfaces with different aIgG surface density onto described PCA model are presented in Fig. 3b as a function of the protein surface density Γ. Each data point represents the average scores value for all spectra recorded from each sample with a given IgG surface density. An analysis of the PC3 scores values provides an insight regarding how the orientation of surface-immobilized aIgG changes with the protein surface density. A flat-on aIgG orientation is expected for the lowest surface coverage, with mass loading values < 1.2 mg/m^2. Then, as the surface density increases (up to 2.2 mg/m^2) a shift of data points to higher PC3 values is observed in Fig. 3b, corresponding to the IgG molecules with the larger ratio $Fc/F(ab)_2$ of the areas of exposed Fc and $F(ab)_2$ domains. This observation is interpreted as adopting of a side-on orientation by aIgG molecules. A related molecular simulation study [14] confirm this interpretation: The ratio $Fc/F(ab)_2$ rises from 0.38 to 0.52 for stable molecular configurations as the orientation changed from flat-on to side-on [14].

A further increase of surface density above 2.2 mg/m^2 results in even stronger shift of data points in Fig. 3b in the direction of positive PC3 values. This suggests a vertical orientation of aIgG molecules with dominant a head-on orientation, characterized by exposed Fc and hidden $F(ab)_2$ domains. For example, the proportion between aIgG molecules adapting head-on and tail-on orientation at the level of 3:1, proposed in Scheme 1b, is characterized by $Fc/F(ab)_2$ ratio equal to 0.67 deduced from [14]. In order to achieve more lucid data visualization and classification, the data points were divided into three groups characterized by flat-on, side-on and head-on dominant orientations versus the protein surface density. The groups defined are marked in Fig. 3b as I, II and III grey rectangles, each with position and height corresponding to mean and standard deviation of PC3 scores of all included TOF-SIMS spectra, respectively. The difference in the mean PC3 scores value between the analyzed groups on a coefficient level 0.05 was confirmed by ANNOVA test.

3.3.2. Surface functionalization with NHS-silane

The scores plot (PC3 vs. PC1) for PCA model developed for TOF-SIMS spectra recorded from molecular layers papered on silicon substrates modified with NHS-silane is presented in Fig. 4a. The interpretation of the first (capturing 68.67% of the variance), second (capturing 18.76% of variance) and third (capturing 3.46% of the variance) principal components is consistent with that for SiO_2 substrates functionalized with APTES/glutaraldehyde. The mean PC3 scores values for all aIgG layers prepared on NHS-silane modified surface are plotted in Fig. 4b versus protein surface density, following the approach described for proteins on surfaces functionalized with aldehyde groups (Fig. 3b). As for aldehyde modified surface, also here the PC3 reveals the changes of aIgG molecules orientation with the increase of protein surface density (Fig. 4b). The flat-on orientation, observed for the lowest mass loadings (up to 1. 3 mg/m^2), changes to a more vertical side-on arrangement that is reflected by the shift of respective data points towards more positive PC3 values. Again, this reflects the immobilized IgG molecule with an increased ratio $Fc/F(ab)_2$ of the areas of exposed Fc and $F(ab)_2$ domains (with a rise from 0.38 to 0.52 deduced from [14]). In turn, for even higher protein surface density, $\Gamma > 2.3$ mg/m^2, a shift of data points in the opposite direction is observed, with the resulting negative PC3 values, slightly lower than the PC3 level obtained for aIgG in flat-on orientation. This indicates a change of aIgG orientation for a vertical one with a significant contribution of a tail-on orientation. For example, a mixed orientation with equal proportions of molecules adapting head-on and tail-on arrangements, as proposed in Scheme 1d, results in a ratio $Fc/F(ab)_2$ of exposed Fc and $F(ab)_2$ fragments equal to 0.34 deduced form [14], that is slightly below the value (0.38) characteristic for aIgG molecules adapting a flat-on orientation. Again, for more lucid data visualization and classification, data points were divided into three groups, marked in Fig. 4b as I, II and III grey rectangles, and the difference in the mean PC3 scores value between them on a coefficient level 0.05 was confirmed by ANNOVA test.

3.3.3. Amino acids characteristic for outermost regions of aIgG layers

In order to relate the result of PCA analysis with differences in amino acid composition of outermost regions of examined protein layers, loadings of particular PCs should be considered. The loadings plots for PC1 are presented in Figs. S3 and S4 in Supplementary Material, while these for PC3 are presented in Fig. 5. It is evident from Fig. 5 that the loadings on PC3 defined by PCA independently for both sample series, corresponding to APTES/glutaraldehyde (Fig. 5a) and NHS-silane modified surfaces (Fig. 5b), show great consistency. This fact ensures the high reliability and correct interpretation of analytical data. An analysis of loadings on PC3 enables disclosure of amino acids characteristic for Fc and $F(ab)_2$ fragments of goat anti-rabbit IgG antibody. Amino acid such as proline (Pro), histidine (His), phenylalanine (Phe) and arginine (Arg) can be identified as characteristic for the Fc fragment of goat IgG, due to distinctly positive loadings values of ions derived from these amino acids. This set of amino acids (except of Arg) is in accordance with results of TOF-SIMS study of mouse IgG [6,20] and its amino acid composition from Protein Data Bank [6,17]. In turn, serine (Ser), asparagine (Asn), threonine (Thr), leucine (Leu) and tryptophan (Trp) are indicated as more prevalent in the fragment $F(ab)_2$ of anti-rabbit goat IgG. Although an exact amino acid sequence of Fab fragment of the antibody used in the current study is not determined, the significantly higher abundance of serine and leucine in Fab than Fc fragment has been reported for other IgG1 molecules [6,16,40].

3.4. aIgG orientation vs. antigen binding efficiency

In order to examine the influence of surface density and orientation of surface-immobilized anti-rabbit goat IgG antibodies (aIgG) on their antigen binding efficiency an immunoreaction with rabbit IgG (rIgG) was performed. The aIgG layers of different surface density prepared on APTES/glutaraldehyde and NHS-silane modified substrates were firstly blocked with BSA to prevent non-specific antigen adsorption. The impact of blocking step on total protein surface density is discussed in Section S5 of Supplementary Material. Then, the samples were incubated in a solution of rabbit IgG and the amount of rIgG bound onto the surface was determined with spectroscopic ellipsometry (Fig. 6a), widely used as a convenient method for label-free biomolecular

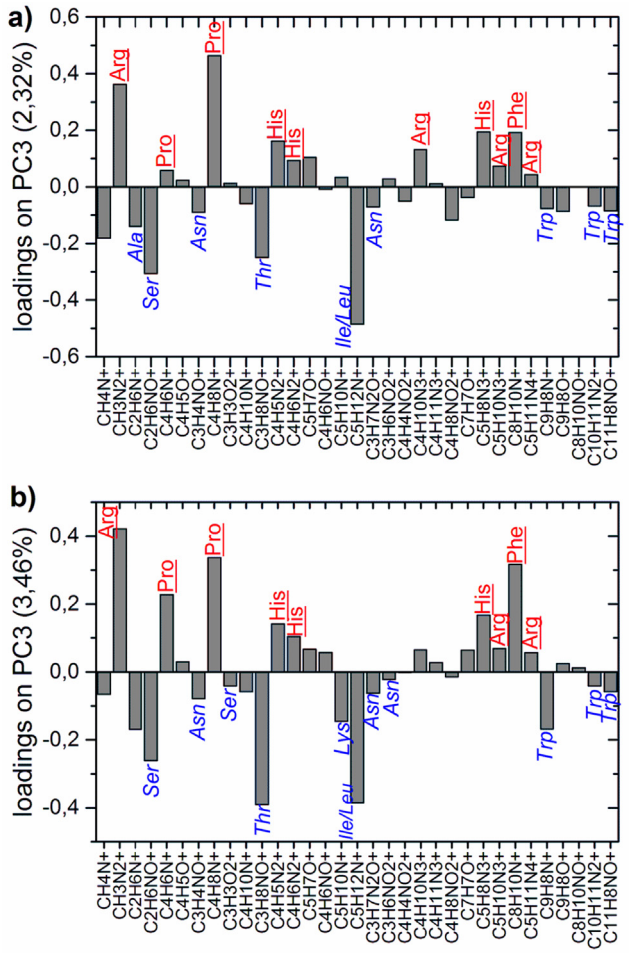

Fig. 5. Loadings plot for the third PC in PCA models developed for TOF-SIMS spectra recorded from aIgG layers immobilized on APTES/glutaraldehyde (a) and NHS-silane (b) functionalized SiO_2 surfaces (Fig. 3a and 4a): ion fragments of amino acids abundant in Fc domain (red underlined) load in the positive direction, while fragments of amino acids with higher content in $F(ab)_2$ domain (blue italic) load in the negative direction.

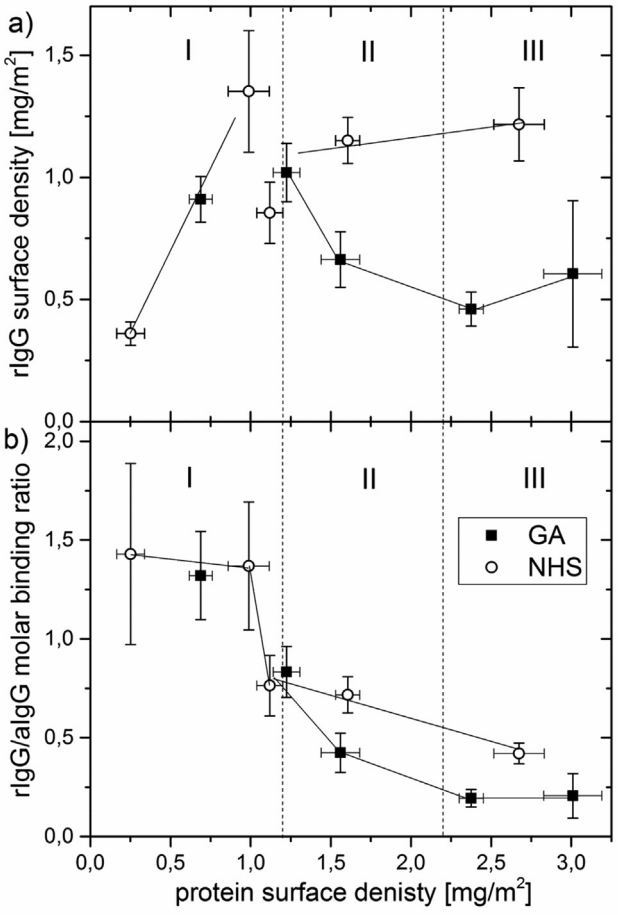

Fig. 6. Analysis of the antigen binding efficiency of aIgG molecules immobilized at different densities on SiO_2 substrates functionalized with NHS-silane (open circles) and APTES/glutaraldehyde (black squares), respectively, with regard to: (a) the amount of bound antigen (rabbit IgG) and, (b) the molar binding ratio of antigen to antibody versus the surface density of aIgG. The surface densities of aIgG and rIgG were determined from ellipsometry measurements. Lines are to guide the eye. Error bars are standard deviations determined from 5 ellipsometry measurements of the same sample.

interaction analysis [3,4,10,20,27,41–44]. The amount of bound antigen was expressed as an increase of protein surface density after immunoreaction compared to the amount of protein onto the surface after the blocking step. In turn, molar binding ratio of the rIgG antigen to the aIgG antibody was determined (Fig. 6b) as the ratio of the amount of bound antigen to the surface density of antibody prior to immunoreaction. Additionally, AFM microscopy was employed to analyze evolution of protein layer upon blocking with BSA and specific antigen binding (Fig. 7).

To examine the effect of antibodies surface density on antigen binding efficiency, the data regarding the amount of rIgG bound onto the surface (Fig. 6a) and the molar binding ratio (Fig. 6b) are considered. As shown in Fig. 6a, the amount of bound antigen initially increases with aIgG surface density (for $\Gamma < 1.2$ mg/m^2, marked as I) reflecting an increase in the amount of binding sites on the surface. In turn, for higher Γ values (marked as II and III), the bound amount of rIgG stops to increase for NHS-silane modified surfaces, and decreases for surfaces modified with APTES/glutaraldehyde. Such a behavior is related to increase of steric hindrance as the surface density of aIgG increases, as well as to changes in aIgG molecules orientation. To draw more clear conclusions regarding the effect of orientation changes, the amount of bound antigen was expressed as binding ratio. As show in Fig. 6b, the antigen binding ratio, plotted as function of antibody surface density Γ (Fig. 6b), decreases in the whole Γ range except for the lowest values [10,42]. For aIgG surface density $\Gamma < 1.2$ mg/m^2 (marked as I in Fig. 6) more than one antigen molecule is bound to each aIgG molecule. This result further confirms a domination of flat-on orientation (as concluded from TOF-SIMS and AFM), in which two antigen binding sites are exposed. The effective prevention of the non-specific antigen adsorption achieved with the blocking procedure even for low surface coverage with aIgG, is confirmed by the results obtained for the reference samples with immobilized Fc fragments ($\Gamma = 1.0 \pm 0.1$ mg/m^2 and $\Gamma = 1.2 \pm 0.2$ mg/m^2 for APTES/glutaraldehyde and NHS-silane surface modification, respectively), where no increase of protein surface density was observed after incubation with antigen solution (See Table S1 in Section S5 in Supplementary Material). It seems, that in contrast to hydrophobic surfaces on which a flat-on antibodies orientation is described as biologically inactive [9,12], the antibodies on SAM modified silicon substrates retain their antigen binding capacity in this orientation. The effective antigen binding by antibodies adopting a flat-on orientation was reported earlier for antibodies adsorbed on silicon dioxide substrate [10,42,43]. Increase of the aIgG surface density above 1.2 mg/m^2 (marked as II in Fig. 6) results in a gradual reduction of the antigen binding ratio due to orientation changes and increasing steric hindrance between adjacent binding sites [10,42]. For Γ values corresponding to a dominant side-on orientation, a molar binding ratio of 0.4–0.7 was estimated that is in

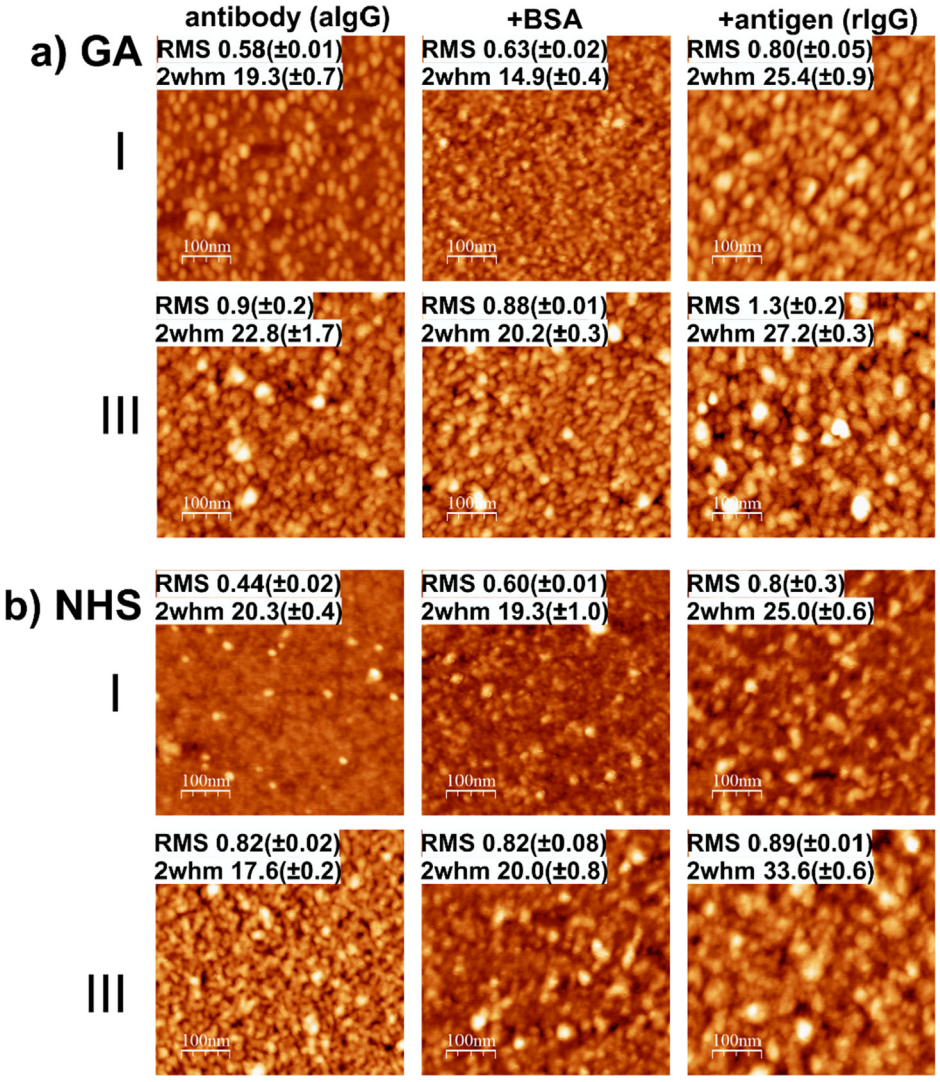

Fig. 7. AFM characterization of the antigen binding to aIgG immobilized on SiO_2 substrates functionalized with (a) APTES/glutaraldehyde or (b) NHS-silane with low ($\Gamma = 0.68 \pm 0.07$ mg/m^2 and 0.25 ± 0.09 mg/m^2 for aldehyde and NHS-modified surfaces, respectively) and high ($\Gamma = 2.38 \pm 0.08$ mg/m^2 and 2.79 ± 0.01 mg/m^2 for aldehyde and NHS-modified surfaces, respectively) surface density corresponding to flat-on (I) and vertical (III) aIgG orientation, respectively. Representative AFM images (with identical height-range of 6 nm) recorded after aIgG immobilization, blocking of free surface sites with BSA, and immunoreaction with rIgG, as well as nanostructure parameters: root mean square roughness RMS [nm] and mean size of surface features 2whm [nm].

accordance with the theoretical maximum value of 1, reflecting binding of antigen to the one binding site exposed in this orientation. Finally, high antibody surface densities $\Gamma > 2.2$ mg/m^2 (marked as III in Fig. 6) are characterized by antigen binding capacity of about 0.2 and 0.4 for APTES/glutaraldehyde and NHS-silane functionalized silicon substrates, respectively. The significantly higher values of the amount of bound antigen and antigen molar binding ratio estimated for high surface density of aIgG immobilized on substrates functionalized with NHS-silane compared to those functionalized with APTES/glutaraldehyde confirms that a greater number of aIgG molecules are adapting an active tail-on orientation on the surface modified with NHS-silane, as concluded from TOF-SIMS analysis (summarized also in Scheme 1b and 1d). The values of antigen binding ratio determined can be also partially affected by the steric hindrance phenomenon, that is particularly prominent for large-sized antigens as IgG, limiting the number of bound antigens [42–44].

To further evaluate the antibody layers structure after antigen binding, AFM microscopy was employed (Fig. 7). The incubation of the aIgG-coated and BSA-blocked surfaces with the rIgG solution results in an increase of the mean surface feature size at least to 25 nm, regardless of the aIgG initial surface density and substrate functionalization strategy. This result confirms the specific antigen binding, since the affinity protein binding is expressed in AFM images as enlargement of surface features [33,41,45,46]. Additionally, the significantly higher size of surface features after rIgG binding to aIgG immobilized with high surface density on NHS-silanized surface (34 nm) compared to APTES/glutaraldehyde modified surface (27 nm) can be interpreted as a more effective antigen binding, indicating a greater share of antibodies adopting a tail-on orientation on the former surface.

3.5. Discussion of surface density induced orientation changes

The surface density ranges determined for different types of aIgG molecule orientation are comparable for both functionalization approaches of silicon substrate examined in the current manuscript and consistent for all the experiments performed. In turn, a difference in proportion of aIgG molecules adapting tail-on and head-on orientation on NHS-ester and aldehyde functionalized silicon surfaces is indicated for high surface density forcing a vertical molecular arrangement. In particular, from TOF-SIMS analysis, supported by antigen binding assay, a dominant head-on orientation is revealed for the substrates modified with APTES/glutaraldehyde, while mixed orientation with a significant share of molecules adopting a tail-on orientation is demonstrated for the substrates modified with NHS-silane (see Scheme 1). One of the major factors determining protein adsorption and affecting antibodies orientation are electrostatic interactions [5,6]. The control of antibodies orientation through interaction between the charge of SAMs and electric IgG dipoles, both induced at neutral pH (by properly adjusted values of acid dissociation constant of SAM, pKa, and isoelectric points of IgG and its Fab and Fc domains), was demonstrated by Chen

for ionic strength much lower than that applied here [5]. In our work, the above mechanism of electrostatic dipole-surface interactions seems not to be crucial, due to low surface charge expected for both types of surface functionalization: Applied buffer pH 7.4 is slightly above pKa values reported for APTES (~6.6–7.3) [47] and may cause only weak protonation of NH_2 groups, along with uncharged (protonated) aldehyde groups. In addition, under such conditions an inefficient hydrolysis of NHS groups, and hence absence of resulting negatively charged COO^- groups, was reported [48]. In contrast, intermolecular dipole–-dipole electrostatic interactions between crowded IgG molecules promote at high Γ values an anti-ferroelectric pattern of alternating protein dipoles corresponding to mixed tail-on/head-on aIgG orientation [49], which is observed on NHS-silane modified surface (Scheme 1d). Basically, protein biding to aldehyde and NHS-terminated SAM occurs by reaction with primary protein amines, such as the N-terminus α-amine (pKa 7.6–8.0) and ε-amine of lysine residues (pKa 9.3–9.5), both reactive in a neutral (or basic) pH [48,50]. However, before their covalent conjugation, the aIgG molecules need to be physisorbed on the surface [3,51,52]. Therefore, we believe that the orientation of aIgG molecules on NHS-silane modified surface reflects alternating arrangement of protein dipoles during physisorption that occurs prior to covalent binding. In turn, on glutaraldehyde modified surface a greater share of molecules adapting head-on orientation is observed (Scheme 1b), with the proportion of antibodies with head-on to tail-on orientation is close to 3:1. The main reason for this could be random immobilization through lysine residues, randomly distributed between the two Fab and the Fc fragments. Additional preference of the head-on orientation could be the result of higher reactivity of α-amine groups of N-terminus, located on Fab domains, with lower pKa values as compared to more protonated ε-amine groups of lysine residues. This result (Scheme 1b) suggests a scenario with a negligible impact of intermolecular interactions on the final arrangement of aIgG molecules immobilized on glutaraldehyde modified surfaces, that could be due to faster protein capture to the surface containing amine groups [51,52]. In fact, the higher binding capacity estimated for glutaraldehyde modified than for NHS-silane modified surfaces could reflect differences in kinetic of protein binding to the modified surfaces. Recent studies on antibodies immobilization report, however without a strict control of surface density, a domination of tail-on alignment on NHS-terminated SAM [17] and head–on [53,54] or random IgG orientation [55,56] on glutaraldehyde modified surfaces, that are in accordance with our observations.

4. Conclusions

The dominant orientation of IgG antibody molecules immobilized by covalent binding on SiO_2 surfaces following two functionalization strategies, namely functionalization with NHS-silane or functionalization with APTES followed by modification with glutaraldehyde, was evaluated for a wide range of antibodies surface density. For this purpose, a complementary analysis with TOF-SIMS spectrometry supported with PCA, AFM imaging and evaluation of the antigen binding efficiency, supplemented by ellipsometric evaluation of protein surface density, was employed.

We demonstrated for the first time that TOF-SIMS with PCA can directly trace changes in the orientation of surface-immobilized antibodies as a function of their surface density. The subsequent transition of the dominant antibodies orientation from flat-on ($\Gamma < 1.2$ mg/m^2) to side-on ($\Gamma = 1.2$–2.2 mg/m^2) and finally a vertical tail-on/head-on orientation ($\Gamma > 2.2$ mg/m^2) as the aIgG surface density Γ increases was revealed.

The determined ranges of mass loading Γ for each particular orientation are different from the values reported earlier based on the assumption of close packing of immobilized proteins [3,5,7,9,11]. Instead, the Γ value ranges determined in the current study correspond to *lower* packing efficiency ('jamming limit' Θ_∞) of individual biomolecules with different dominant orientations. This points to Random Sequential Adsorption as more appropriate than Langmuir model to describe protein adsorption. In Langmuir model each molecule can adsorb to *one* discrete surface site, so additional molecules can be adsorbed even when almost all surface sites are covered by already bound proteins [57]. Therefore *high* packing efficiency cannot be excluded (for assumed close-packed arrangement). However, each real protein is large enough to occupy numerous sites of a *continuous* surface [57]. Also, each already adsorbed molecule excludes from further adsorption a region, due to repulsive protein–protein interactions, with the same center and doubled molecular diameter [31,35,57]. RSA model shows that sequentially adsorbed molecules [57] form a randomly packed protein monolayer with *lower* packing efficiency given by Θ_∞ [58]. Surface exclusion effects described by RSA model are not taken properly into account by Langmuir model [57], even when it is extended [57] to impose 'jamming limit' Θ_∞ on discrete surface sites. Still, extended Langmuir model is a useful reference [35], applied also here along with RSA to analyze adsorption isotherms of aIgG on glutaraldehyde and NHS-silane modified surfaces.

The PCA analysis performed allows also for identification of the dominant orientation (tail-on vs. head-on) for vertically oriented aIgG. It was revealed that at high surface density values, the immobilized antibodies prefer a head-on orientation on glutaraldehyde modified surfaces, while a significant percentage of molecules are adopting a tail-on orientation on the NHS-silane modified surfaces. Additionally, the calculated antigen binding capacity, as described by the molar binding ratio of antigen to antibody, reveals a reduction with increasing aIgG mass loading due to both orientation changes and increased steric hindrance. Thus, the optimum surface density of aIgG molecules, resulting in the maximum amount of bound antigen, is estimated as 1.0–1.2 mg/m^2. The complex analysis of the orientation of aIgG immobilized on silanized silicon substrates, described in this paper, juxtaposed with their biological activity, can be applied to optimize the procedures for immunosensors functionalization for various applications.

CRediT authorship contribution statement

Katarzyna Gajos: Supervision, Conceptualization, , Investigation, Data curation, Writing - original draft. **Klaudia Szafraniec:** Investigation. **Panagiota Petrou:** Validation, Writing - review & editing. **Andrzej Budkowski:** Methodology, Validation, Data curation, Visualization, Writing - original draft.

Declaration of Competing Interest

The authors declare that they have no known competing financial interests or personal relationships that could have appeared to influence the work reported in this paper.

Acknowledgments

This work was financed by Polish National Science Center (NCN) under Grant 2016/21/N/ST5/00880. K.G. is grateful for financial support from the Foundation for Polish Science (FNP) (in the framework of the START scholarship).

Appendix A. Supplementary material

Additional information and data on: i) models describing adsorption isotherms; ii) surface sensitivity of TOF-SIMS; iii) AFM characterization of aIgG layers; iv) TOF-SIMS and PCA analysis of the aIgG orientation and v) ellipsometry analysis of the blocking step of binding assay. Supplementary data to this article can be found online at https://doi.org/10.1016/j.apsusc.2020.146269.

References

[1] T.R.J. Holford, F. Davis, S.P.J. Higson, Recent trends in antibody based sensors, Biosens. Bioelectron. 34 (2012) 12–24.
[2] S.C.B. Gopinath, T.H. Tang, M. Citartan, Y. Chen, T. Lakshmipriya, Current aspects in immunosensors, Biosens. Bioelectron. 57 (2014) 292–302.
[3] A.K. Trilling, J. Beekwilder, H. Zuilhof, Antibody orientation on biosensor surfaces: a minireview, Analyst 138 (2013) 1619–1627.
[4] N.G. Welch, J.A. Scoble, B.W. Muir, P.J. Pigram, Orientation and characterization of immobilized antibodies for improved immunoassays (Review), Biointerphases 12 (2017) 02D301.
[5] S. Chen, L. Liu, J. Zhou, S. Jiang, Controlling antibody orientation on charged self-assembled monolayers, Langmuir 19 (2003) 2859–2864.
[6] H. Wang, D.G. Castner, B.D. Ratner, S. Jiang, Probing the orientation of surface-immobilized immunoglobulin G by time-of-flight secondary ion mass spectrometry, Langmuir 20 (2004) 1877–1887.
[7] J. Buijs, D.D. White, W. Norde, The effect of adsorption on the antigen binding by IgG and its F(ab')2 fragments, Coll. Surf. B 8 (1997) 239–249.
[8] J. Buijs, J.W.T. Lichtenbelt, W. Norde, J. Lyklema, Adsorption of monoclonal IgGs and their F(ab′) < inf > 2 < /inf > fragments onto polymeric surfaces, Coll. Surf. B 5 (1995) 11–23.
[9] M.E. Wiseman, C.W. Frank, Antibody adsorption and orientation on hydrophobic surfaces, Langmuir 28 (2012) 1765–1774.
[10] X. Zhao, F. Pan, B. Cowsill, J.R. Lu, L. Garcia-Gancedo, A.J. Flewitt, G.M. Ashley, J. Luo, Interfacial immobilization of monoclonal antibody and detection of human prostate-specific antigen, Langmuir 27 (2011) 7654–7662.
[11] H. Chen, J. Huang, J. Lee, S. Hwang, K. Koh, Surface plasmon resonance spectroscopic characterization of antibody orientation and activity on the calixarene monolayer, Sensors Actuators, B Chem. 147 (2010) 548–553.
[12] C. Dupont-Gillain, Orientation of adsorbed antibodies: In situ monitoring by QCM and Random sequential adsorption modeling, ACS Symp. Ser. 1120 (2012) 453–469.
[13] A. Makky, T. Berthelot, C. Feraudet-Tarisse, H. Volland, P. Viel, J. Polesel-Maris, Substructures high resolution imaging of individual IgG and IgM antibodies with piezoelectric tuning fork atomic force microscopy, Sensors Actuators, B Chem. 162 (2012) 269–277.
[14] J.G. Vilhena, A.C. Dumitru, E.T. Herruzo, J.I. Mendieta-Moreno, R. Garcia, P.A. Serena, R. Pérez, Adsorption orientations and immunological recognition of antibodies on graphene, Nanoscale 8 (2016) 13463–13475.
[15] H. Xu, X. Zhao, C. Grant, J.R. Lu, D.E. Williams, J. Penfold, Orientation of a monoclonal antibody adsorbed at the solid/solution interface: A combined study using atomic force microscopy and neutron reflectivity, Langmuir 22 (2006) 6313–6320.
[16] F. Liu, M. Dubey, H. Takahashi, D.G. Castner, D.W. Grainger, Immobilized antibody orientation analysis using secondary ion mass spectrometry and fluorescence imaging of affinity-generated patterns, Anal. Chem. 82 (2010) 2947–2958.
[17] V. Lebec, S. Boujday, C. Poleunis, C.-M. Pradier, A. Delcorte, Time-of-flight secondary ion mass spectrometry investigation of the orientation of adsorbed antibodies on sams correlated to biorecognition tests, J. Phys. Chem. C. 118 (2014) 2085–2092.
[18] N.G. Welch, R.M.T. Madiona, T.B. Payten, C.D. Easton, L. Pontes-Braz, N. Brack, J.A. Scoble, B.W. Muir, P.J. Pigram, Surface immobilized antibody orientation determined using ToF-SIMS and multivariate analysis, Acta Biomater. 55 (2017) 172–182.
[19] J.-W. Park, I.-H. Cho, D.W. Moon, S.-H. Paek, T.G. Lee, ToF-SIMS and PCA of surface-immobilized antibodies with different orientations, Surf. Interface Anal. 43 (2011) 285–289.
[20] K. Gajos, A. Budkowski, V. Pagkali, P. Petrou, M. Biernat, K. Awsiuk, J. Rysz, A. Bernasik, K. Misiakos, I. Raptis, S. Kakabakos, Indirect immunoassay on functionalized silicon surface: molecular arrangement, composition and orientation examined step-by-step with multi-technique and multivariate analysis, Coll. Surf. B. 150 (2016) 437–444.
[21] K. Awsiuk, A. Budkowski, P. Petrou, M.M. Marzec, M. Biernat, T. Jaworska-Gołąb, J. Rysz, Orientation and biorecognition of immunoglobulin adsorbed on spin-cast poly(3-alkylthiophenes): Impact of polymer film crystallinity, Coll. Surf. B. 148 (2016) 278–286.
[22] Y. Stetsyshyn, J. Raczkowska, A. Budkowski, A. Kostruba, K. Harhay, H. Ohar, K. Awsiuk, A. Bernasik, N. Ripak, J. ZemŁa, Synthesis and postpolymerization modification of thermoresponsive coatings based on pentaerythritol monomethacrylate: surface analysis, wettability, and protein adsorption, Langmuir 31 (2015) 9675–9683.
[23] D. Duval, A.B. González-Guerrero, S. Dante, C. Domínguez, L.M. Lechuga, Interferometric waveguide biosensors based on Si-technology for point-of-care diagnostic, in: Proc. SPIE - Int. Soc. Opt. Eng., 2012, pp. 8431P.
[24] G. Gauglitz, Point-of-care platforms, 7 (2014) 297–315.
[25] J.A. Howarter, J.P. Youngblood, Optimization of silica silanization by 3-aminopropyltriethoxysilane, Langmuir 22 (2006) 11142–11147.
[26] J. Kim, J. Cho, P.M. Seidler, N.E. Kurland, V.K. Yadavalli, Investigations of chemical modifications of amino-terminated organic films on silicon substrates and controlled protein immobilization, Langmuir 26 (2010) 2599–2608.
[27] P.A. Cuypers, J.W. Corsel, M.P. Janssen, J.M. Kop, W.T. Hermens, H.C. Hemker, The adsorption of prothrombin to phosphatidylserine multilayers quantitated by ellipsometry, J. Biol. Chem. 258 (1983) 2426–2431.
[28] I. Horcas, R. Fernández, J.M. Gómez-Rodríguez, J. Colchero, J. Gómez-Herrero, A.M. Baro, WSXM: A software for scanning probe microscopy and a tool for nanotechnology, Rev. Sci. Instrum. 78 (2007) 013705.
[29] L.C.L. Aquino, E.A. Miranda, I.S. Duarte, P.T.V. Rosa, S.M.A. Bueno, Adsorption of human immunoglobuling onto ethacrylate and histidine-linked methacrylate, Brazilian J. Chem. Eng. 20 (2003) 251–262.
[30] B.M. Manzi, M. Werner, E.P. Ivanova, R.J. Crawford, V.A. Baulin, Simulations of protein adsorption on nanostructured surfaces, Sci. Rep. 9 (2019) 1–13.
[31] Z. Adamczyk, Modeling adsorption of colloids and proteins, Curr. Opin. Colloid Interface Sci. 17 (2012) 173–186.
[32] R.E. Ducker, M.T. Montague, G.J. Leggett, A comparative investigation of methods for protein immobilization on self-assembled monolayers using glutaraldehyde, carbodiimide, and anhydride reagents, Biointerphases 3 (2009) 59–65.
[33] K. Awsiuk, A. Budkowski, P. Petrou, A. Bernasik, M.M. Marzec, S. Kakabakos, J. Rysz, I. Raptis, Model immunoassay on silicon surfaces: Vertical and lateral nanostructure vs. protein coverage, Coll. Surf. B. 103 (2013) 253–260.
[34] K. Awsiuk, A. Budkowski, A. Psarouli, P. Petrou, A. Bernasik, S. Kakabakos, J. Rysz, I. Raptis, Protein adsorption and covalent bonding to silicon nitride surfaces modified with organo-silanes: Comparison using AFM, angle-resolved XPS and multivariate ToF-SIMS analysis, Coll. Surf. B. 110 (2013) 217–224.
[35] M. Rabe, D. Verdes, S. Seeger, Understanding protein adsorption phenomena at solid surfaces, Adv. Colloid Interface Sci. 162 (2011) 87–106.
[36] K. Awsiuk, A. Budkowski, M.M. Marzec, P. Petrou, J. Rysz, A. Bernasik, Effects of polythiophene surface structure on adsorption and conformation of bovine serum albumin: A multivariate and multitechnique study, Langmuir 30 (2014) 13925–13933.
[37] S. Muramoto, J. Brison, D.G. Castner, Exploring the surface sensitivity of TOF-secondary ion mass spectrometry by measuring the implantation and sampling depths of Bi n and C 60 ions in organic films, Anal. Chem. 84 (2012) 365–372.
[38] K. Gajos, M. Angelopoulou, P. Petrou, K. Awsiuk, S. Kakabakos, W. Haasnoot, A. Bernasik, J. Rysz, M.M. Marzec, K. Misiakos, I. Raptis, A. Budkowski, Imaging and chemical surface analysis of biomolecular functionalization of monolithically integrated on silicon Mach-Zehnder interferometric immunosensors, Appl. Surf. Sci. 385 (2016) 529–542.
[39] M.S. Wagner, D.G. Castner, Characterization of adsorbed protein films by time-of-flight secondary ion mass spectrometry with principal component analysis, Langmuir 17 (2001) 4649–4660.
[40] E. Kosobrodova, R.T. Jones, A. Kondyurin, W. Chrzanowski, P.J. Pigram, D.R. Mckenzie, M.M.M. Bilek, Orientation and conformation of anti-CD34 antibody immobilised on untreated and plasma treated polycarbonate, Acta Biomater. 19 (2015) 128–137.
[41] K. Gajos, A. Budkowski, Z. Tsialla, P. Petrou, K. Awsiuk, P. Dąbczyński, A. Bernasik, J. Rysz, K. Misiakos, I. Raptis, S. Kakabakos, Contact pin-printing of albumin-fungicide conjugate for silicon nitride-based sensors biofunctionalization: Multi-technique surface analysis for optimum immunoassay performance, Appl. Surf. Sci. 410 (2017) 79–84.
[42] H. Xu, J.R. Lu, D.E. Williams, Effect of surface packing density of interfacially adsorbed monoclonal antibody on the binding of hormonal antigen human chorionic gonadotrophin, J. Phys. Chem. B. 110 (2006) 1907–1914.
[43] X. Wang, Y. Wang, H. Xu, H. Shan, J.R. Lu, Dynamic adsorption of monoclonal antibody layers on hydrophilic silica surface: A combined study by spectroscopic ellipsometry and AFM, J. Colloid Interface Sci. 323 (2008) 18–25.
[44] O. Svensson, T. Arnebrant, Antibody-antigen interaction on polystyrene: An in situ ellipsometric study, J. Colloid Interface Sci. 368 (2012) 533–539.
[45] K. Awsiuk, A. Bernasik, M. Kitsara, A. Budkowski, P. Petrou, S. Kakabakos, S. Prauzner-Bechcicki, J. Rysz, I. Raptis, Spectroscopic and microscopic characterization of biosensor surfaces with protein/amino-organosilane/silicon structure, Coll. Surf. B. 90 (2012) 159–168.
[46] K. Gajos, P. Petrou, A. Budkowski, K. Awsiuk, A. Bernasik, K. Misiakos, J. Rysz, I. Raptis, S. Kakabakos, Imaging and spectroscopic comparison of multi-step methods to form DNA arrays based on the biotin-streptavidin system, Analyst 140 (2015) 1127–1139.
[47] K. Van Der Maaden, K. Sliedregt, A. Kros, W. Jiskoot, J. Bouwstra, Fluorescent nanoparticle adhesion assay: A novel method for surface pK a determination of self-assembled monolayers on silicon surfaces, Langmuir 28 (2012) 3403–3411.
[48] P. Wagner, M. Hegner, P. Kernen, F. Zaugg, G. Semenza, Covalent immobilization of native biomolecules onto Au(111) via N- hydroxysuccinimide ester functionalized self-assembled monolayers for scanning probe microscopy, Biophys. J. 70 (1996) 2052–2066.
[49] E.N. Vasina, P. Déardin, Adsorption of α-chymotrypsin onto mica in laminar flow conditions. Adsorption kinetic constant as a function of tris buffer concentration at pH 8.6, Langmuir 20 (2004) 8699–8706.
[50] M. Mentinova, N.Z. Barefoot, S.A. McLuckey, Solution versus gas-phase modification of peptide cations with NHS-ester reagents, J. Am. Soc. Mass Spectrom. 23 (2012) 282–289.
[51] C. Mateo, G. Fernández-Lorente, O. Abian, R. Fernández-Lafuente, J.M. Guisán, Multifunctional epoxy supports: A new tool to improve the covalent immobilization of proteins. The promotion of physical adsorptions of proteins on the supports before their covalent linkage, Biomacromolecules 1 (2000) 739–745.
[52] C. Mateo, R. Torres, G. Fernández-Lorente, C. Ortiz, M. Fuentes, A. Hidalgo, F. López-Gallego, O. Abian, J.M. Palomo, L. Betancor, B.C.C. Pessela, J.M. Guisan, R. Fernández-Lafuente, Epoxy-amino groups: A new tool for improved immobilization of proteins by the epoxy method, Biomacromolecules 4 (2003) 772–777.
[53] G.-Y. Liu, N.A. Amro, Positioning protein molecules on surfaces: A nanoengineering approach to supramolecular chemistry, Proc. Natl. Acad. Sci. 99 (2002) 5165–5170.
[54] K. Wadu-Mesthrige, N.A. Amro, J.C. Garno, S. Xu, G.Y. Liu, Fabrication of nanometer-sized protein patterns using atomic force microscopy and selective

immobilization, Biophys. J. 80 (2001) 1891–1899.
[55] T.Q. Huy, N.T.H. Hanh, P. Van Chung, D.D. Anh, P.T. Nga, M.A. Tuan, Characterization of immobilization methods of antiviral antibodies in serum for electrochemical biosensors, Appl. Surf. Sci. 257 (2011) 7090–7095.
[56] Y. Yuan, M. Yin, J. Qian, C. Liu, Site-directed immobilization of antibodies onto blood contacting grafts for enhanced endothelial cell adhesion and proliferation, Soft Matter 7 (2011) 7207–7216.
[57] P. Schaaf, J. Talbot, Surface exclusion effects in adsorption processes, J. Chem. Phys. 91 (1989) 4401–4409.
[58] E.L. Hinrichsen, J. Feder, T. Jøssang, Geometry of random sequential adsorption, J. Stat. Phys. 44 (1986) 793–827.